Hydrogen Atom Mediated Stone−Wales Rearrangement of Pyracyclene: A Model for Annealing in Fullerene Formation

Mark R. Nimlos*

National Renewable Energy Laboratory, Golden, Colorado 80401

Jonathan Filley and J. Thomas McKinnon

Department of Chemical Engineering, Colorado School of Mines, Golden, Colorado 80401

Received: June 24, 2005; In Final Form: August 25, 2005

We have investigated the Stone−Wales (SW) rearrangement of pyracyclene ($C_{14}H_{12}$) using quantum mechanical molecular modeling. Of particular interest in this study is the effect of an added hydrogen atom on the barriers to SW rearrangement. Hydrogen atoms are found in high abundance during combustion, and their effect upon isomerization of aromatic compounds to more stable species may play an important role in the combustion synthesis of fullerenes. We have calculated the barriers for the SW rearrangement in pyracyclene using density functional theory B3LYP/6-31G(d) and B3LYP/6-311G(d,p). Two mechanisms have been investigated: (i) a mechanism with two identical transition states of C_1 symmetry and a cyclobutyl intermediate and (ii) a mechanism with one transition state containing an sp^3 carbon (*J. Am. Chem. Soc.* **2003**, *125*, 5572−5580; *Nature* **1993**, *366*, 665−667). We find that the barriers for these mechanisms are 120.0 kcal mol^{-1} for the cyclobutyl mechanism and 130.1 kcal mol^{-1} for the sp^3 mechanism. Adding a hydrogen atom to the internal bridge carbon atoms of pyracyclene reduces the barrier of the cyclobutyl mechanisms to 67.0 kcal mol^{-1} and the sp^3 mechanism to 73.1 kcal mol^{-1}. The bonding of carbon atoms in pyracyclene is similar to those found in isomers of C_{60}, and the barriers are low enough so that these reactions can become significant during fullerene synthesis in flames. Adding hydrogen atoms to the external bridge atoms on pyracyclene produces a smaller reduction in the SW barrier and adding hydrogen atoms to nonbridge external carbon atoms results in no reduction of the barrier.

Introduction

Fullerenes are formed readily in both carbon electric arcs[3,4] and in flames.[5,6] The process clearly involves molecular weight growth reactions, which form large, spherical carbon networks from smaller carbon fragments; in the case of electric arcs, these fragments consist of carbon radicals of variable size, while in the case of flames, they consist of carbon radicals, hydrocarbon radicals, and stable molecules, such as acetylene. In addition to growth processes, there must occur a great deal of carbon atom network rearrangement in order to arrive at a stable fullerene such as buckminsterfullerene (BF, C_{60}). This molecule is notable since only one isomer out of the 1811 possibilities[7] has been isolated. In this isomer all the five-membered rings are surrounded by six-membered rings, with the carbon atoms forming a truncated icosahedron, the same geometry found in soccer balls. It has been widely postulated that the formation of BF relies on the rearrangement of higher energy isomers with nonisolated pentagons.[8] It has also been postulated that this rearrangement occurs with the carbon atoms adjusting smoothly while remaining embedded in the fullerene framework via a diradical type of transition state, which is the original Stone−Wales (SW) reaction,[9,10] or via a carbene intermediate,[2,11] where one carbon atom makes a brief excursion beyond the periphery of the forming BF during the reaction. Calculations on BF suggest that the activation barriers for the carbene pathway are lower[1,2] and range from 132 to 170 kcal mol^{-1}. The transition state for the original SW mechanism is over 40 kcal mol^{-1} higher.

These high activation barriers are problematic for two reasons. First, even the lower calculated energy barrier is greater than the bond dissociation energy of the C−C bonds in BF. Thus, destruction of the carbon network would be a lower energy pathway relative to the SW network rearrangement making the SW pathway appear unlikely to occur if such high barriers are correct. The second conundrum is related to the rate at which this reaction can occur. Fullerenes form in flames at approximately 2000 K at an upper limit time constant of 5 ms—the residence time in a fullerene-producing flame.[12] If we assume that the reaction is first order with an upper limit *A*-factor of 1×10^{16} s^{-1} (an extremely high value for a reaction with a tight transition state) then the half-life for a single SW rearrangement would be approximately 30 s—several orders of magnitude longer than the flame residence time. We were prompted by these two observations to search for other fullerene network rearrangement pathways that might be operative in flames. Since the temperatures in electric arcs are much higher than flames, the SW rearrangement may well be operative in that environment.

Another difference in flames relative to a carbon arc, in addition to the reduced temperature, is that there is a major difference in the chemical environment. The flame environment is one of small unsaturated hydrocarbons (C_2H_2, etc.), polycyclic aromatic hydrocarbons, CO, H_2, and an abundant concentration

* To whom correspondence should be addressed.

10.1021/jp053441j CCC: $30.25
Published on Web 10/06/2005

of small and large free radicals.[13] For example, hydrogen atom mole fractions exceed 1% in fullerene-producing flames.[14] The plentiful concentration of radicals led us to consider a radical-mediated Stone−Wales isomerization process in which radicals play a role in the intermediates. Specifically we considered only an H atom mediated Stone−Wales rearrangement due to the relative dominance of H atoms as well as its high reactivity toward unsaturated species.

Theoretical studies of radical pathways in fullerene formation have been performed on BF (as C_{61})[15] and on fullerene fragments,[8] and the researchers have found barriers substantially lower than 160 kcal mol^{-1} using a variety of radicals. While important, these studies utilized somewhat limited theoretical methods, due to the size of the molecules under investigation. It is therefore important to perform higher level theoretical studies on the radical-mediated pathways to fullerenes.

Herein we present density functional computational results on the smallest molecule that in principle can undergo a bona fide Stone−Wales rearrangement, pyracyclene (**1**), and reactions 1 and 2, with special emphasis on the radical-mediated reaction using hydrogen atom, one of the most abundant radicals found in flames. It is crucial to bear in mind that we are using pyracyclene as a model compound to illustrate the possible isomerization pathways for fullerenes and large fullerene fragments. The intermediates and transition states in this paper are probably never formed in the thermal reactions of pyracyclene, at least for the nonradical pathways, since the work of Scott, et al.,[16] indicates there is *zero* evidence that the SW reaction occurs in pyracyclene or other polycyclic aromatic hydrocarbons (PAH). Nevertheless, the structures in and the energetics of the reaction pathways presented here are directly relevant to the relative lowering of barrier heights that is achieved when a SW rearrangement is mediated by a radical. Extension of this work to larger systems, and to BF itself, will provide further computational data on the complex topic of the mechanism of fullerene formation.

Computational Details

We have chosen pyracyclene (with 14 heavy atoms) as a model system for the SW reaction because it has four rings whose ring sizes are affected by the rearrangement and because it contains a structural motif of C_{60}. Two mechanisms for the SW rearrangement were investigated in this study, mechanisms 1 and 2. Mechanism 1 is a new mechanism and is here referred to as the **cyclobutyl mechanism**. It is a two-step mechanism consisting of a cyclobutyl intermediate, **3**, of C_{2h} symmetry and two mirror-image transition states, **2**, of C_1 symmetry. Mechanism 2, a concerted reaction, was proposed by Scuseria et al.[1,2] and using their nomenclature, is referred to as the **sp**^{3} mechanism. This mechanism involves a single transition state, **4**, of C_s symmetry. We were not successful in our attempts to obtain another transition state of C_2 symmetry as proposed earlier[1,2,9] for SW in C_{60}, mechanism 3. The cyclobutyl mechanism (mechanism 1) is represented in reaction 1 for the neat pyracyclene case and in reactions 4 and 6 for the hydrogen-mediated case. The sp^3 mechanism (mechanism 2) is represented for neat pyracyclene in reaction 2 and for the hydrogen-mediated case in reactions 5 and 7.

Pyracyclene, D_{2h} symmetry, has eight external carbon atoms (C1−C8), four identical atoms on the C_5 rings (C1, C2, C5, and C6) and four on the C_6 rings (C3, C4, C7, and C8). During the SW reaction the external carbon atoms exchange from C_5 rings to C_6 rings. The four identical external bridge carbon atoms (C9−C12) in pyracyclene remain at the external bridges after

Mechanisms 1: cyclobutyl mechanism

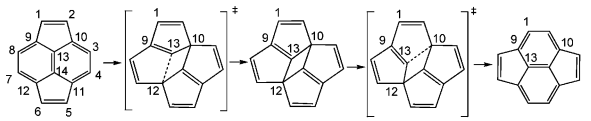

(1)

D_{2h} C_1 C_{2h} C_1 D_{2h}

1 **2** **3** **2** **1**

Mechanism 2: sp^3 mechanism

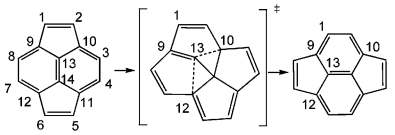

(2)

D_{2h} C_s D_{2h}

1 **4** **1**

Mechanism 3 (TS not found)

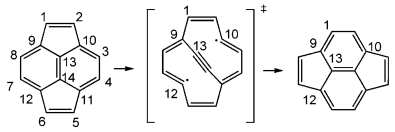

(3)

C_2 not found

the SW reaction, but two of them change bonding to the internal bridge atoms (C13 and C14) as shown in reaction 1. For instance, during the SW reaction, C13 breaks its bond with C10 and forms a bond with C12. Similarly, C14 breaks the bond with C12 and forms a bond with C10.

The choice of this model system allows us to use a reasonably accurate level of density functional theory and a large enough basis set (B3LYP/6-31G(d)) to obtain fairly accurate molecular geometries and energies. Calculated energies at this level of the theory have a standard deviation from experiment of 9.5 kcal mol^{-1} using the G2 molecule set.[17] We used this technique to survey the energetics of the SW reaction when a hydrogen atom is added at different positions on pyracyclene. In a few cases, we have conducted more accurate calculations using a triple-ζ basis set, 6-311G(d,p). B3LYP with this basis set provides a standard of deviation of about 3.1 kcal mol^{-1} for the G2 molecule set.[17] Because B3LYP/6-311G(d,p) is more computationally intensive, we limited these calculations to neat pyracyclene and pyracyclene with a hydrogen atom added to the internal bridge carbon atoms, C13 and C14. We found the largest reduction in the SW barriers when a hydrogen atom was added to these positions. The accuracy of the energies obtained for transition states using the theoretical techniques in this study are not as well characterized as for stable molecules. There are several studies[18−22] that show that B3LYP typically underpredicts transition state energies by approximately 5 kcal mol^{-1}.

The calculations in this study were carried out using the Gaussian 98 suite of programs[23] performed on an IBM RS/6000, Sun Ultra 80 (NREL), or SGI cluster (NCSA) systems. Local minima and transitions states were found using Berny optimizations. Starting geometries for the transition state optimizations were often located using a potential energy scan, where one internal coordinate was systematically changed while all other coordinates where allowed to relax. The geometry at the calculated maximum of this scan was used as a starting geometry for a transition state optimization. Stable structures had only positive vibrational frequencies while transition states had one imaginary frequency. The transition states were confirmed by

SCHEME 1

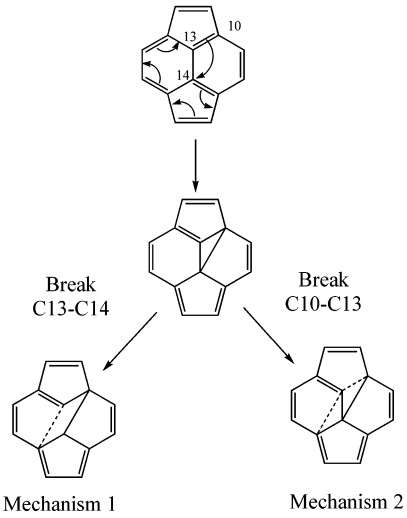

visual inspection of the imaginary frequency and by the use of IRC calculations.[24,25]

Results and Discussion

Cyclobutyl Mechanism. Mechanism 1 features the surprising step of breaking the central bond between C13 and C14 and then re-forming it in the product. While one might expect this to be a higher energy pathway compared to the sp^3 mechanism, in which the C13−C14 bond remains intact, the differences between the mechanisms are relatively minor. In fact, the cyclobutyl pathway was found to be energetically more favorable than the sp^3 pathway, as discussed below. The beginning step of the two pathways is shown formally in Scheme 1, where a cyclopropane ring is formed by the concerted motion of 10 electrons. Depending on which bond of the cyclopropane ring is then broken, the reaction leads to the cyclobutyl or the sp^3 mechanism. It should be emphasized that computationally the cyclopropane compound is more like a transition state (see below) which can lead to the cyclobutyl intermediate or to the sp^3 transition state on the potential energy surface, and is misrepresented as a stable compound in Scheme 1 in order to illustrate the changes in bonding that occur in the two mechanisms.

Stone—Wales Isomerization in Neat Pyracyclene. To set the baseline for the hydrogen atom mediated SW reaction in pyracyclene, we first conducted calculations on the SW reaction of neat pyracyclene. Using B3LYP/6-31G(d), transition states were successfully obtained for mechanism 1 and mechanism 2, shown in reactions 1 and 2. As mentioned above, we were not successful in obtaining the transition state for SW isomerization proposed earlier that is shown in reaction 3. The energy of this transition state was shown by others in earlier work to be about 40 kcal mol^{-1} higher in energy than the barrier for the sp^3 mechanism,[2] and is not considered to be likely. The energetics of the SW reaction for neat pyracyclene are collected in Table 1 together with those for the hydrogen-mediated SW rearrangement. More accurate energies for the SW reaction of neat pyracyclene were obtain using B3LYP/6-311G(d,p) and the results of these calculations are plotted in Figure 1. At the B3LYP/6-311G(d,p) level energy barriers for these two mechanisms are similar, though the barrier of the cyclobutyl mechanism, $E_0(\mathbf{2}) = 120.0$ kcal mol^{-1}, is lower than the barrier for the sp^3 mechanism, $E_0(\mathbf{3}) = 130.1$ kcal mol^{-1}. This latter value is consistent to that obtained earlier[2] using BLYP/SCF, $E_0 = 140.5$ kcal mol^{-1}. These activation energies are large compared to the bond energy of a single carbon bond (i.e., for ethane[26] $\Delta H_{298} = 90$ kcal mol^{-1}) and are comparable to a

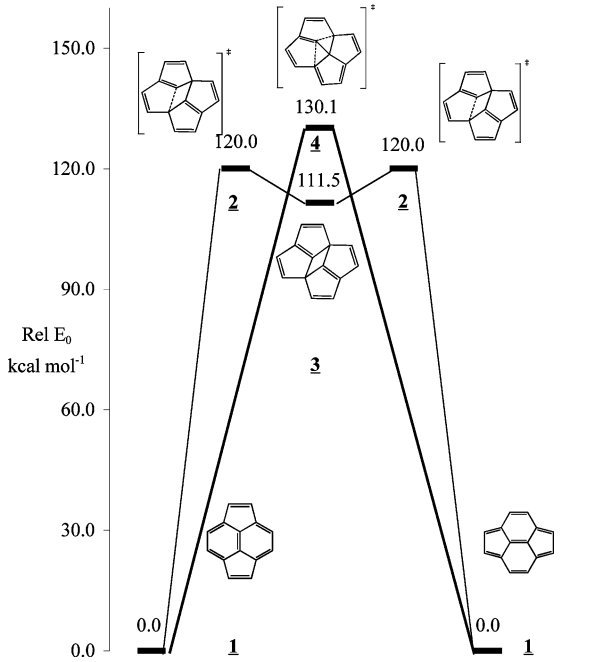

Figure 1. Potential energies for Stone−Wales rearrangement of pyracyclene calculated using B3LYP/6-311G(d,p).

TABLE 1: Calculated Energies[a] of SW Reaction for Neat Pyracyclene and Pyracyclene after Hydrogen Atom Addition (kcal mol^{-1})

	energies relative to reactant adduct[b]						
	cyclobutyl mechanism				sp^3 mechanism		
	reaction	E_0(TS)	E_0(cyclobutyl)	E_0(TS)	reaction	E_0(TS)	E_0(product)
pyracyclene neat	1	121.7 (**2**)	112.9 (**3**)		2	131.8 (**4**)	0.0[d]
H-inner bridge: **A1**	4	66.9 (**9**)	65.4 (**11**)		5	73.3 (**12**)	0.0[d]
		NA (**10**)					
H-outer bridge: **A2**	6	105.3 (**13**)	97.4 (**15**)		7	101.4 (**16**)	0.0[c]
		122.8 (**14**)				134.8 (**17**)	
						118.6 (**18**)	
H-external: **A3** → **A4**[d]	8	133.0 (**19**)	118.8 (**23**)	131.4 (**21**)	10	137.3 (**29**)	14.6 (**A4**)
		128.0 (**20**)		125.9 (***22***)		127.7 (***30***)	
	9	139.2 (**24**)	133.9 (**28**)	NA (**26**)		NA (**31**)	
		142.2 (**25**)		142.8 (**27**)		132.9 (**32**)	

[a] B3LYP/6-31G(d), energies include zero point energy. [b] Calculated energies relative to the reactant as shown in the text. For instance, for reaction 4 the energies are relative to **5**. [c] For these reactions, the products are identical to the reactants. [d] Structures for these species and the corresponding reactions are found in the Supporting Information.

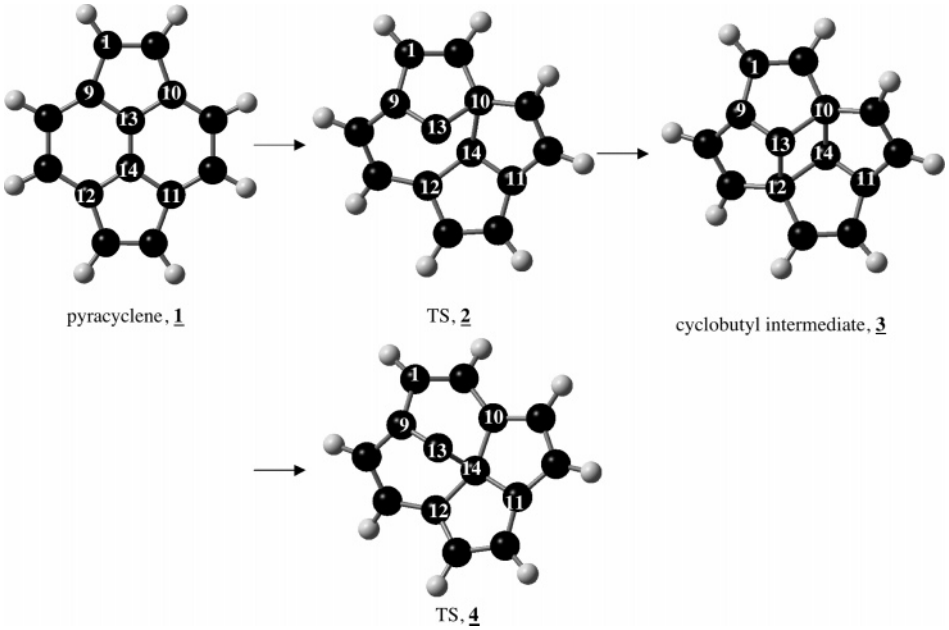

Figure 2. Molecular structures for the SW rearrangement of pyracyclene, **1**. The transition state for cyclobutyl mechanism, **2** and the cyclobutyl, **3**, intermediated are shown at the top and transition state for sp^3 mechanism, **4** is shown at the bottom. Lengths of the carbon−carbon bonds are collected in Table 2.

TABLE 2: Bond Lengths[a] for Reactions 1, 2, 4 and 5 (See Figures 2 and 4)

	neat pyracyclene					pyracyclene + H on C13			
	1	**1** (exptl[b])	**2**	**3**	**4**	**5**	**9**	**11**	**12**
	D_{2h}	D_{2h}	C_1	C_{2h}	C_s	C_1	C_1	C_1	C_1
C1−C2	1.37	1.346	1.36	1.36	1.37	1.44	1.36	1.36	1.37
C3−C4	1.45	1.443	1.36		1.40	1.40	1.36	1.36	1.40
C5−C6			1.39			1.38	1.38		
C7−C8			1.37				1.36		
C1−C9	1.49	1.492	1.45	1.45	1.46	1.39	1.44	1.44	1.45
C2−C10			1.48	1.49	1.44		1.49	1.50	1.46
C3−C10	1.39	1.379	1.49		1.42	1.43	1.48	1.48	1.42
C4−C11			1.45		1.41	1.43	1.44	1.45	1.41
C5−C11			1.42			1.47	1.42		
C6−C12			1.44				1.45		
C7−C12			1.45				1.47		
C8−C9			1.43				1.43		
C9−C13	1.41	1.397	1.40	1.39	1.38	1.49	1.50	1.51	1.50
C10−C13			1.50	1.57	2.03		1.56	1.62	2.05
C10−C14			1.60		1.56		1.56	1.55	1.52
C11−C14			1.41		1.46	1.39	1.42	1.40	1.48
C12−C13			1.51				1.85		
C12−C14			1.99				1.52		
C13−C14	1.35	1.360	1.66		1.45	1.44	1.77		1.49

[a] From B3LYP/6-311G(d,p). Redundant lengths due to symmetry are not listed. [b] Reference 27.

delocalized double bond (i.e., for butadiene[26] $\Delta H_{298} = 116$ kcal mol^{-1}). That is, the localization of this much energy in an individual bond would more likely lead to bond rupture and destruction of the aromatic network than isomerization into a fullerene structure.

Bond length analysis of both transition states show that there is significant double bond character in the bond between C9 and C13 as shown in reactions 1 and 2. Figure 2 shows the structure of pyracyclene and the reaction intermediates in reactions 1 and 2 and Table 2 contains the C−C bond lengths. The experimental bond lengths for pyracyclene[27] are shown in the column next to the calculated values. The calculated bond lengths are within 0.025 Å of the experimental values, and as these bond lengths show, there is considerable delocalization of the π electrons throughout the carbon structure. These bond lengths are all shorter than typical single bonds, 1.52−1.53 Å,[28] and larger than typical double bonds, 1.33−1.35 Å.[29]

For the cyclobutyl mechanism, the sp^2 hybridization of C13 and C14 and the π character of the C9−C13 and C11−C14 bonds create strain on the cyclobutyl ring and account for the high energy of the transition state and the cyclobutyl intermediate. Because of the planarity of the rest of the periphery carbon atoms, the bond angles involving C13 and C14 are significantly distorted from the value of 120° typically found for sp^2 carbon atoms. For instance, for the cyclobutyl intermediate, **3**, the C10−C13−C12 bond angle is 109°, closer to the bond angle of a typical sp^3 carbon atom.

For the sp^3 transition state, **4**, the short bond distance between C13 and C9, 1.38 Å, suggests that there is also significant double bond character between these atoms. As with the TS for the cyclobutyl mechanism, the bonding to C13, which is formally sp^2 hybridized, is significantly distorted from planarity, with the C13−C14 bond roughly 63° out of the plane formed by C13, C9, and C1. The severe distortion of the sp^2 hybridized carbon atom at C13 in both mechanisms, which gives rise to the high activation energy, leads to the possibility that attachment of a hydrogen atom at this site with the corresponding change in hybridization to sp^3, will relieve the strain and lower the activation barrier.

Hydrogen-Mediated Stone−Wales Pyracyclene Isomerization. The calculations in this study show that the addition of a hydrogen atom to pyracyclene can increase the likelihood of the SW rearrangement by lowering the reaction barriers for the mechanisms in reactions 1 and 2. The SW reaction barriers for the pyracyclene/hydrogen atom adduct are strongly dependent upon the location of hydrogen atom addition on the pyracyclene, with addition to C13 producing the largest decrease in the barrier, about 50−60 kcal mol^{-1}. There is a smaller reduction in the barrier when the hydrogen atom adds at C9, and virtually no reduction in the barrier when hydrogen atom adds to the other nonbridging carbon atoms.

The reaction of H + pyracyclene leads to different adducts (**A1**−**A4**) depending on the site of addition. The mechanistic

discussion below is restricted to reactions leading to adducts **A1** and **A2** because these have relevance to fullerenes (which have only internal sites). There was very little reduction in the SW energy barrier from the addition to the external carbon atoms, adducts **A3** and **A4**, so those routes are not discussed in detail below. However, data for reactions leading to **A3** and **A4** are included in the tables and figures for completeness and data on adducts **A3** and **A4** is included in the Supporting Information. Key: **A1**, internal bridge carbon atoms (C13, C14); **A2**, external bridge carbon atoms (C9, C10, C11, C12) site; **A3**, external carbon atoms on five-carbon rings (C1, C2, C5, C6); **A4**, external carbon atoms on six-carbon rings (C3, C4, C7, C8).

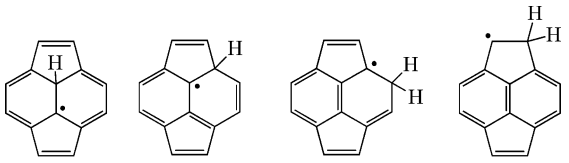

A1 (**5** - C_s) A2 (**6** – C_1) A3 (**7** – C_s) A4 (**8** – C_s)

As with pyracyclene, the π electrons in these molecules are delocalized over the sp^2 carbon atoms. The carbon atom that is the site of hydrogen atom addition becomes sp^3 hybridized, and as a result the carbon framework of adducts **A1** and **A2** are nonplanar. Addition of a hydrogen atom to the external carbon atoms (**A3** and **A4**) does not affect the planarity of the carbon atoms, and these molecules have C_s symmetry.

The SW reaction for adducts **A1** and **A2** lead to products that are identical to the reactant, while the SW reaction of adduct **A3** leads to **A4** and vice versa. For isomers of C_{60}, where only internal bridge carbon atoms exist, only adducts similar to **A1** are possible. The other types of adducts would only be possible for SW reactions involving fragments of C_{60}, such as might be found during combustion synthesis.

Where possible, we have obtained SW transition states for all of these adducts and calculated the energy barriers of reactions as well as the reaction energies. The calculated relative energies for the SW reactions of pyracyclene/hydrogen atom adducts are compared to neat pyracyclene in Table 1. These energies were determined at the B3LYP/6-31G(d) level. The first column lists the reaction number in the text for the cycyclobutyl mechanisms, the second column lists the relative energy of transition state, E_0(TS), for this mechanism, and the third column lists the relative energy of the cyclobutyl intermediate, E_0(cyclobutyl). Columns five and six show the reaction number and transition state energy for the sp^3 mechanisms. Descriptions of the mechanisms for the reaction in this table are provided below. We were not able to find geometries for some of the possible transition states shown below.

The possible pathways for the SW reaction involving the **A1** adduct formed by addition to the inner carbon atom are shown in reactions 4 and 5 for the cyclobutyl mechanism and the sp^3 mechanism, respectively. The symmetries of the species in these reactions are shown underneath the structures. On the basis of the bonding of transition state **2** for the cyclobutyl mechanism, one could anticipate four distinct transition states for this mechanism, which are shown. Note that the two transition states labeled **9** are mirror images of each other, as are those labeled **10**, but that **9** and **10** are structural isomers because different bonds are breaking and forming with respect to the radical center. In practice, we could identify only one transition state **9**. Transition state **10** could not be located, perhaps due to the fact that the distance between C13 and C14 is only 1.66 Å for neat pyracyclene (see Figure 2 and Table 2), suggesting there is significant cyclopropyl character in the transition state, and adding the hydrogen atom as shown in **10** would create a partially pentavalent carbon atom at C13. Transition state **9** and the cyclobutyl intermediate have their unpaired electron delocalized over the top half of the molecule, as shown in reaction 4.

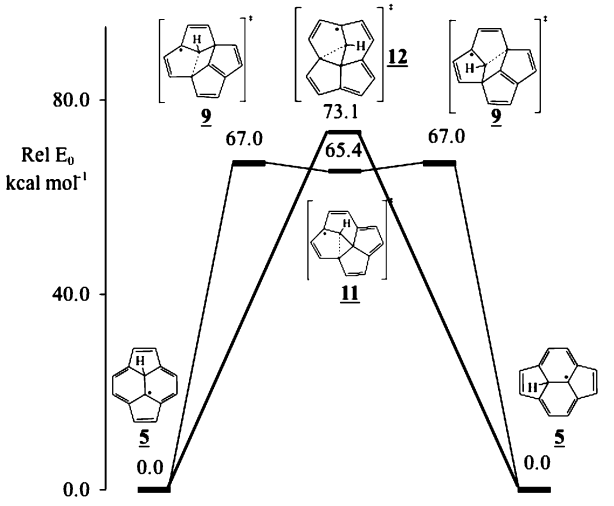

Figure 3. Potential energies for Stone−Wales rearrangement of pyracyclene with the addition of a hydrogen atom to the internal bridge carbon atom calculated using B3LYP/6-311G(d,p).

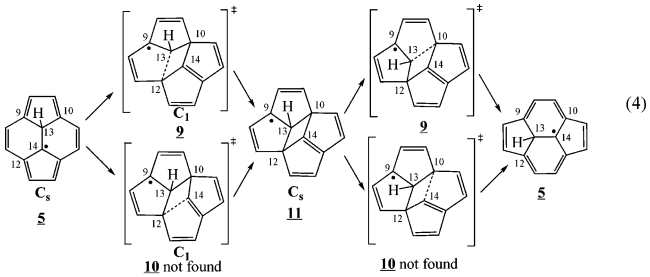

(4)

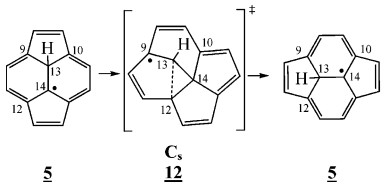

(5)

As Table 1 shows, the relative energies of the transition states in reactions 4 and 5 are significantly lower than the corresponding barriers for neat pyracyclene at the B3LYP/6-31G(d) level. Figure 3 presents a plot of the potential energies reactions 4 and 5 that were calculated using B3LYP/6-311G(d,p) and that include zero point energy. As is seen, the calculated barrier at this higher level for the cyclobutyl mechanism is 67.0 kcal mol^{-1} and the barrier for the sp^3 mechanism is 73.1 kcal mol^{-1}. These barriers are nearly 60 kcal mol^{-1} lower than for the neat pyracyclene and are low enough to be significant at combustion temperatures. In addition, the chemical activation energy from the formation of the C−H bond, amounting to E_0(adduct) = −20.4 kcal mol^{-1}, should be available for surmounting the SW reaction barrier under combustion conditions.

Figure 4 shows the structures of the adduct **A1**, the cyclobutyl transition state, the cyclobutyl intermediate and the sp^3 transition state for SW reaction. For both the transition state, **9**, and the cyclobutyl intermediate, **11**, (see also reaction 4) the radical is delocalized over the carbon atoms of the adjacent double bonds.

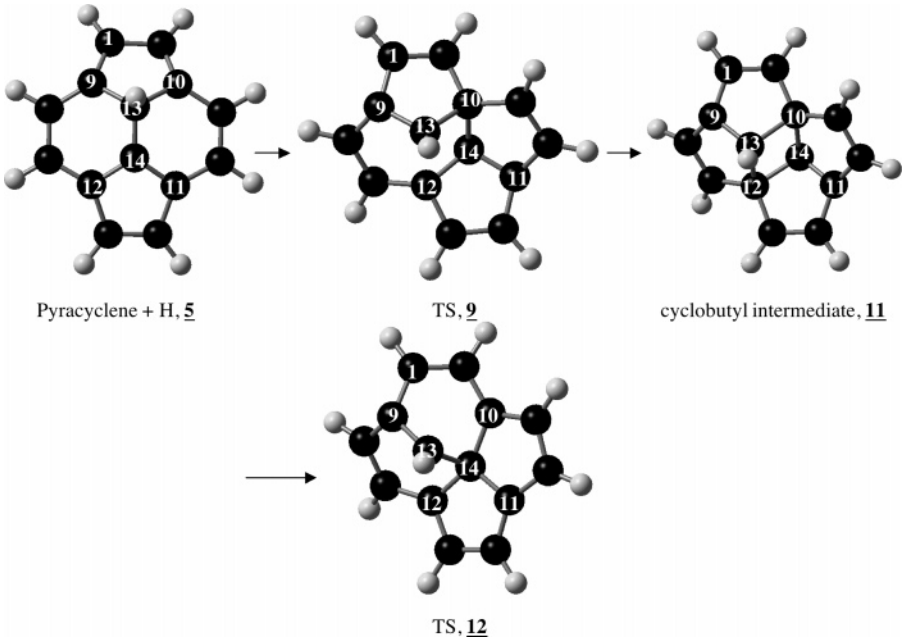

Figure 4. Calculated structures for adduct **A1**, its transition states and intermediates during the Stone−Wales reaction. Carbon−carbon bond lengths are collected in Table 2.

In the transition state the internal bridge carbon atom with the added hydrogen atom, C13, becomes sp^3, as is indicated by the long bond between C9 and C13, $r_{C9-C13} = 1.50$ Å. This bond length is typical[28] for C−C single bonds, where the carbon atoms are sp^3 hybridized. Likewise, the long bond in the cyclobutyl intermediate, $r_{C9-C13} = 1.51$ Å, suggests that C13 is sp^3 hybridized in this molecule. There is only one transition state, **12**, for the sp^3 mechanism, which is shown in reaction 5 and Figure 4. The unpaired electron and π electrons from the periphery carbon atoms are delocalized throughout the external carbon framework, while C13 has become sp^3, as indicated by the long C9−C13 bond, $r_{C9-C13} = 1.50$ Å. In adduct **A1**, hydrogen atom addition significantly reduces the barrier for the SW reaction in both mechanisms, because the resulting sp^3 hybridization at C13 relieves strain in the transition states and intermediates.

For adduct **A2**, formed by addition to the external bridge carbon atom, there are two transition states, **13** and **14**, for the cylobutyl mechanism in reaction 6 and three transition states, **16**−**18**, for the sp^3 mechanism in reaction 7. The transition states for the cyclobutyl mechanism are C_1 symmetry, while the cyclobutyl intermediate, **15**, is C_s symmetry. For the cyclobutyl mechanism the radical is not delocalized in the transition states or the cyclobutyl intermediate because it is surrounded by sp^3 hybridized carbon atoms.

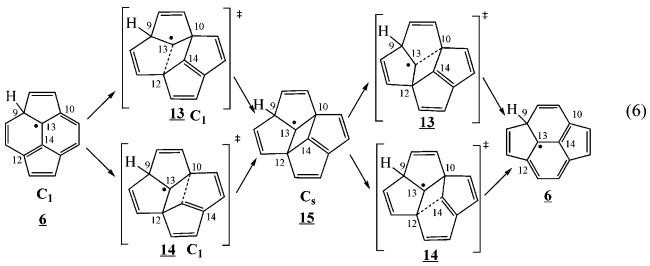

(6)

The two transition states **13** and **14** are differentiated by where the added hydrogen atom is relative to the reacting carbon atom, or the carbon atom that is forming a bond to give the cyclobutyl intermediate. In transition state **13**, the added hydrogen atom is in the β position, while for **14** it is on the other side of the molecule from the reacting atoms. In **13**, the radical is on the reacting carbon atom, while in **14** the radical is on the opposite side of the cyclobutyl ring. As can be seen from Table 1, the energy barrier for reaction 6 is lower for transition state **13**, $E_a = 105.3$ kcal mol^{-1}, than it is for **14**, $E_a = 122.8$ kcal mol^{-1}. The low barrier for **13** is likely due to the formation of a radical at the reacting carbon. This forces C13 to have sp^3 character and relieves the strain on the cyclobutyl transition state. This barrier is lower than the barrier for neat pyracyclene, reaction 1, but is higher than the barrier when H atom is added to the internal bridge carbon atoms, reaction 4. The barrier for reaction 6, transition state **13**, is higher than for reaction 4 because the unpaired electron in **13** cannot delocalize to the same extent as can occur for **9**. In **9**, the unpaired electron has a double allylic structure, while for **13** there are no adjacent double bonds. The barrier for reaction 6 is lower than the bond energy of resonantly stabilized C−C bonds, but is comparable to the bond energy of C−C single bonds. Thus, this reaction may occur in molecules where there is delocalization of π electrons and no single bonds. The adduct energy, E_0(adduct) = −34.5 kcal mol^{-1}, will also be available for reaction of the adduct.

Of the three transition states shown for the sp^3 mechanism only **16** produces a significant decrease in the energy barrier for reaction 7 relative to the SW reaction of neat pyracyclene, reaction 2. Transition state **18** produces a small reduction in the barrier (13.2 kcal mol^{-1}), and the reason for this is unclear, though this apparent change may be within the uncertainty of the computational technique. As with the cyclobutyl mechanism, the lowest barrier is obtained for the transition state with the hydrogen atom added in the β position relative to C13. This forces C13 to be sp^3 hybridized and relieves strain in the transition state. The barrier for this reaction with transition state **13** is $E_a = 101.4$ kcal mol^{-1}, and while this is lower than the SW barrier for neat pyracyclene, it is higher than the SW barrier when a hydrogen atom is added to the internal bridge carbon atom, C13. As with the cyclobutyl mechanism, this is due to reduced resonance stabilization of the radical. For **16**, the radical cannot be resonantly stabilized because it is surrounded by sp^3

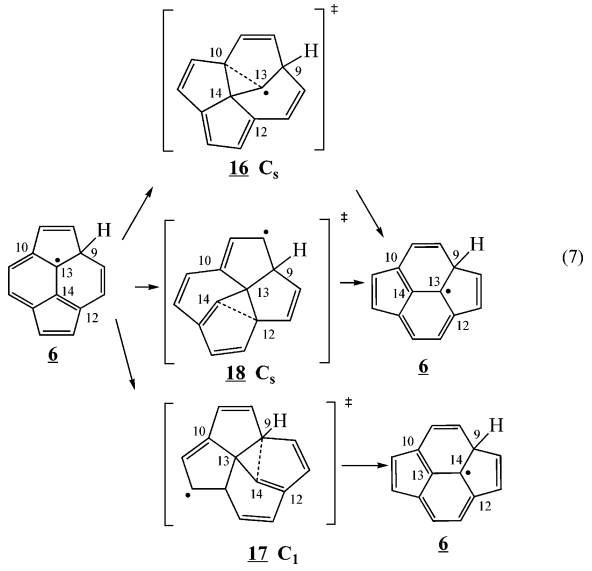

(7)

hybridized carbon atoms. For transition states **17** and **18** the radical is delocalized over the external carbon atom network, but C13 is sp^3 hybridized and experiences similar strain as found in the transition state of the neat pyracyclene reaction, and the barriers for reaction with these transition states is $E_a = 134.8$ kcal mol^{-1} and $E_a = 118.6$ kcal mol^{-1}.

The cases of radical addition to nonbridging carbon atoms (adducts **A3** and **A4**) were also investigated. The reductions in the activation barriers relative to the neat case were very small so they are not reported here in detail. The activation barriers are summarized in Tables 1 and 3 and in Figure 5; the full details are in the Supporting Information.

The SW energy barriers for the pyracyclene reaction after adding a hydrogen atom are summarized in Figure 5. This figure shows the structures for the two transition states for neat pyracyclene and the numbers indicate the SW reaction barrier when a hydrogen atom is added to different positions. As can be seen, significant reduction in the SW barrier only occurs when hydrogen atom adds to the reacting carbon atom (C13) or the carbon atom that is in the β position relative to the reacting carbon (C9). This is because addition at these locations leads to sp^3 character in the reacting carbon atom, which relieves the strain of the transition state. The increase in sp^3 character of this atom is reflected in the bond length to the β carbon atom. Table 3 compares this bond length for all of the hydrogen atom adducts, and also displays the activation energies. As can be seen, the SW barrier is lowered relative to neat pyracyclene when this bond length is near 1.5 Å, which is the length of a typical of single C−C bond. For bond lengths shorter than this, there is more double bond character, which leads to more strain in the transition state and a higher SW barrier.

Conclusion

We have shown computationally that a new mechanism for the SW rearrangement of pyracyclene, which features a cyclobutyl intermediate, has a lower barrier than the previously studied sp^3 mechanism. Both mechanisms involve relatively severe distortions of the 120 degree bond angles of the starting material during the reaction, which imparts strain energy to the transition state, and causes high activation energies. The addition of hydrogen atom to the reacting centers, and to a lesser extent to carbon atoms β to the reacting centers, relieves this strain and lowers the activation energies by as much as 45%. Since the high temperatures found during the typical synthesis conditions of fullerenes lead to an abundance of radicals, especially in flames, it is possible that many fullerene reactions that have been considered as nonradical reactions may in fact occur through radical pathways. The annealing process, in particular the SW reaction, can proceed readily with the activation energies found here if radicals attach themselves to the fullerene surfaces, in analogy to the internal bridge adduct **A1**. In this situation, the half-life for the SW reaction, at 2000 K and assuming a reasonable first-order *A*-factor of 1×10^{13} s^{-1}, is on the order of 2 μs—much faster than the residence time in a flame. Higher level computations will be needed to determine whether the cyclobutyl or the sp^3 mechanism is operative on the surface of an actual curved fullerene, but the results presented here suggest that radicals most likely play an important role in high-temperature fullerene synthesis.

TABLE 3: Comparison of C−C Bond Lengths[a] in the Transition States and SW Reaction Barrier[b] for Pyracyclene and Pyracyclene/Hydrogen Atom Adducts

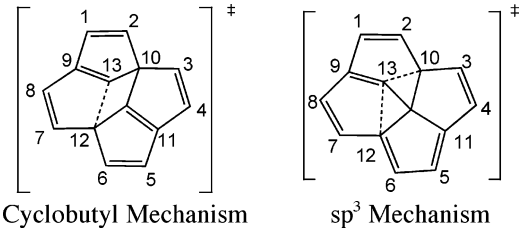

	cyclobutyl mechanism			sp^3 mechanism		
		r (Å)	E_a (kcal mol^{-1})		r (Å)	E_a (kcal mol^{-1})
pyracyclene neat	**2**	1.405	121.7	**4**	1.380	131.8
H-inner bridge: **A1**	**9**	1.494	66.9	**12**	1.496	73.3
H-outer bridge: **A2**	**13**	1.534	105.3	**17**	1.542	101.4
	14	1.392	122.8	**18**	1.418	118.6
				16	1.462	134.8
H external[c]	**19**	1.447	133.0	**29**	1.476	137.3
	20	1.465	128.0	**30**	1.379	127.7
	21	1.461	131.4	**32**	1.365	132.9
	22	1.433	125.9			
	24	1.399	139.2			
	25	1.391	142.2			
	27	1.411	142.8			

[a] Bond lengths are for the bond equivalent to the C9−C13 bond in the transition state of neat pyracyclene. [b] B3LYP/6-31G(d). [c] Structures for these species are found in the Supporting Information.

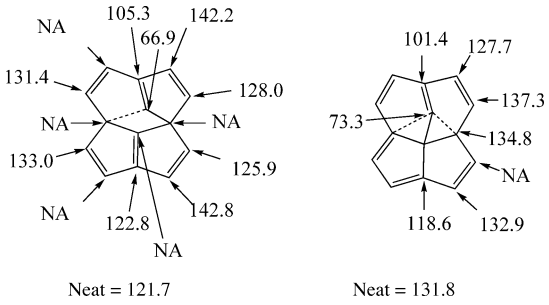

Figure 5. Activation energies, in kcal mol^{-1}, for SW reaction for pyracyclene/hydrogen atom adducts. The values show the calculated, B3LYP/6-31G(d), activation energies for SW for a hydrogen atom added at that position for mechanism 1 (left) and mechanism 2 (right).

Acknowledgment. This work was supported by a grant from the National Center for Supercomputer Applications (NCSA Grant No. CHE-980028n).

Supporting Information Available: Figures showing the cyclobutyl mechanism for **A3** and **A4** and the sp^3 mechanism for **A3** and **A4** and tables of energy and structural data for **1**−**9**, **11**−**25**, **27**, **29**, and **30**. This material is available free of charge via the Internet at http://pubs.acs.org.

References and Notes

(1) Bettinger, H. F.; Yakobson, B. I.; Scuseria, G. E. Scratching the surface of buckminsterfullerene: The barriers for Stone−Wales transformation through symmetric and asymmetric transition states. *J. Am. Chem. Soc.* **2003**, *125*, 5572−5580.

(2) Murry, R. L.; Strout, D. L.; Odom, G. K.; Scuseria, G. E. Role of Sp(3) Carbon and Seven-Membered Rings in Fullerene Annealing and Fragmentation. *Nature* **1993**, *366*, 665−667.

(3) Huczko, A.; Lange, H.; Byszewski, P.; Poplawska, M.; Starski, A. Fullerene formation in carbon arc: Electrode gap dependence and plasma spectroscopy. *J. Phys. Chem. A* **1997**, *101*, 1267−1269.

(4) Guo, T.; Nikolaev, P.; Rinzler, A. G.; Tomanek, D.; Colbert, D. T.; Smalley, R. E. Self-Assembly of Tubular Fullerenes. *J. Phys. Chem.* **1995**, *99*, 10694−10697.

(5) Howard, J. B.; McKinnon, J. T.; Makarovsky, Y.; Lafleur, A. L.; Johnson, M. E. Fullerenes C60 and C70 in Flames. *Nature* **1991**, *352*, 139−141.

(6) Richter, H.; Labrocca, A. J.; Grieco, W. J.; Taghizadeh, K.; Lafleur, A. L.; Howard, J. B. Generation of higher fullerenes in flames. *J. Phys. Chem. B* **1997**, *101*, 1556−1560.

(7) Iijima, S.; Wakabayashi, T.; Achiba, Y. Structures of carbon soot prepared by laser ablation. *J. Phys. Chem.* **1996**, *100*, 5839−5843.

(8) Kroto, H. W. The Stability of the Fullerenes C-24, C-28, C-32, C-36, C-50, C-60 and C-70. *Nature* **1987**, *329*, 529−531.

(9) Stone, A. J.; Wales, D. J. Theoretical-Studies of Icosahedral C60 and Some Related Species. *Chem. Phys. Lett.* **1986**, *128*, 501−503.

(10) Walsh, T. R.; Wales, D. J. Relaxation dynamics of C-60. *J. Chem. Phys.* **1998**, *109*, 6691−6700.

(11) Boorum, M. M.; Vasil'ev, Y. V.; Drewello, T.; Scott, L. T. Groundwork for a rational synthesis of C-60: Cyclodehydrogenation of a C60H30 polyarene. *Science* **2001**, *294*, 828−831.

(12) Richter, H.; Grieco, W. J.; Howard, J. B. Formation mechanism of polycyclic aromatic hydrocarbons and fullerenes in premixed benzene flames. *Combust. Flame* **1999**, *119*, 1−22.

(13) Richter, H.; Howard, J. B. Formation of polycyclic aromatic hydrocarbons and their growth to soot—a review of chemical reaction pathways. *Prog. Energy Combust. Sci.* **2000**, *26*, 565−608.

(14) Bittner, J. D., Howard, J. B. Structure of Sooting Flames. In *Soot in Combustion Systems and its Toxic Properties*; Lahaye J., Prado, G., Eds.; Plenum Press: New York, 1983

(15) Homann, K. H. Fullerenes and soot formation—New pathways to large particles in flames. *Angew. Chem., Int. Ed.* **1998**, *37*, 2435−2451.

(16) Scott, L. T. Fragments of fullerenes: Novel syntheses, structures and reactions. *Pure Appl. Chem.* **1996**, *68*, 291−300.

(17) Foresman, J. B.; Frisch, Æ. *Exploring Chemistry with Electronic Structure Methods*, 2nd ed.; Gaussian Inc.: Pittsburgh, PA, 1995.

(18) Hodgson, D.; Zhang, H. Y.; Nimlos, M. R.; McKinnon, J. T. Quantum chemical and RRKM investigation of the elementary channels of the reaction C6H6+O(P-3). *J. Phys. Chem. A* **2001**, *105*, 4316−4327.

(19) Bach, R. D.; Glukhovtsev, M. N.; Gonzalez, C.; Marquez, M.; Estevez, C. M.; Baboul, A. G.; Schlegel, H. B. Nature of the transition structure for alkene epoxidation by peroxyformic acid, dioxirane, and dimethyldioxirane: A comparison of B3LYP density functional theory with higher computational levels. *J. Phys. Chem. A* **1997**, *101*, 6092−6100.

(20) Basch, H.; Hoz, S. Ab initio study of hydrogen abstraction reactions. *J. Phys. Chem. A* **1997**, *101*, 4416−4431.

(21) Oie, T.; Topol, I. A.; Burt, S. K. Ab Initio and Density-Functional Studies on Internal-Rotation and Corresponding Transition-States in Conjugated Molecules. *J. Phys. Chem.* **1995**, *99*, 905−915.

(22) Dobbs, K. D.; Dixon, D. A. Ab Initio Prediction of the Activation-Energy for the Abstraction of a Hydrogen-Atom from Methane by Chlorine Atom. *J. Phys. Chem.* **1994**, *98*, 12584−12589.

(23) Frisch, M. J.; Trucks, G. W.; Schlegel, H. B.; Scuseria, G. E.; Robb, M. A.; Cheeseman, J. R.; Zakrzewski, V. G.; Montgomery, J. A., Jr.; Stratmann, R. E.; Burant, J. C.; Dapprich, S.; Millam, J. M.; Daniels, A. D.; Kudin, K. N.; Strain, M. C.; Farkas, O.; Tomasi, J.; Barone, V.; Cossi, M.; Cammi, R.; Mennucci, B.; Pomelli, C.; Adamo, C.; Clifford, S.; Ochterski, J.; Petersson, G. A.; Ayala, P. Y.; Cui, Q.; Morokuma, K.; Malick, D. K.; Rabuck, A. D.; Raghavachari, K.; Foresman, J. B.; Cioslowski, J.; Ortiz, J. V.; Stefanov, B. B.; Liu, G.; Liashenko, A.; Piskorz, P.; Komaromi, I.; Gomperts, R.; Martin, R. L.; Fox, D. J.; Keith, T.; Al-Laham, M. A.; Peng, C. Y.; Nanayakkara, A.; Gonzalez, C.; Challacombe, M.; Gill, P. M. W.; Johnson, B. G.; Chen, W.; Wong, M. W.; Andres, J. L.; Head-Gordon, M.; Replogle, E. S.; Pople, J. A. *Gaussian 98*, revision 98; Gaussian Inc.: Pittsburgh, PA, 1998.

(24) Gonzalez, C.; Schlegel, H. B. Reaction-Path Following in Mass-Weighted Internal Coordinates. *J. Phys. Chem.* **1990**, *94*, 5523−5527.

(25) Gonzalez, C.; Schlegel, H. B. An Improved Algorithm for Reaction-Path Following. *J. Chem. Phys.* **1989**, *90*, 2154−2161.

(26) Blanksby, S. J.; Ellison, G. B. Bond dissociation energies of organic molecules. *Acc. Chem. Res.* **2003**, *36*, 255−263.

(27) Freiermuth, B.; Gerber, S.; Riesen, A.; Wirz, J.; Zehnder, M. Molecular and electronic structure of pyracylene. *J. Am. Chem. Soc.* **1990**, *112*, 738−44.

(28) The C−C bond length in ethane is 1.5351 Å, the C−C bond length in propane is 1.532 Å, and the central C−C bond length in *n*-butane is 1.531 Å.[30]

(29) The experimental carbon−carbon double bond length is 1.339 Å for ethylene,[31] 1.353 Å for propylene,[31] 1.342 Å for 1-butene,[32] 1.346 Å for 2-butene-(*Z*),[32] 1.347 Å for 2-butene-(*E*),[32] 1.338 Å for 2-pentene-(*Z*),[33] and 1.334 Å for 2-pentene-(*E*).[33]

(30) Kuchitsu, K., Ed. *Structure of Free Polyatomic Molecules-Basic Data*; Springer: Berlin, 1998.

(31) Herzberg, G. *Electronic spectra and Electronic Structure of Polyatomic Molecules*; Van Nostrand: New York, 1966.

(32) Hellwege, K. H., Hellwege, A. M. Eds. *Landolt-Bornstein: Group II: Atomic and Molecular Physics*; Springer-Verlag, Berlin, 1976; Volume 7, Structure Data of Free Polyatomic Molecules.

(33) Kuchitsu, Ed. *Landolt-Bornstein: Group II: Atomic and Molecular Physics*; Springer-Verlag: Berlin, 1987; Volume 15, Structure Data of Free Polyatomic Molecules.